2016 IEEE International Conference on Robotics and Automation (ICRA)
Stockholm, Sweden, May 16-21, 2016

Single Image based Camera Calibration and Pose Estimation of the End-effector of a Robot

R. A. Boby, S. K. Saha

Abstract— **A new method is proposed for measurement of six dimensional pose of an industrial robot using a single image from a camera which is not pre-calibrated. Additionally during the pose determination, camera internal parameters are also obtained, which makes the method a suitable alternative for calibrating camera using a single image. Results from the two variants of the proposed approach are compared with Zhang's camera calibration algorithm and has been found to be better. Another utility of the proposed algorithm is to measure six dimensional pose of an industrial robot. Robot repeatability was also measured using the proposed camera calibration algorithm. The repeatability results were compared with the measurements using Artificial Reality toolkit ArUco which is a de-facto standard in the pose measurements using camera. The performance of the proposed method is better than that obtained from ArUco. Another area of application is identification of kinematic parameters. Using the circle point analysis method, identification of KUKA KR5 Arc robot was done using the proposed method.**

I. Introduction

Measurement of a pose for an industrial robot is necessary for its calibration and performance measurements [1, 2]. The standard methods often involve using Laser Trackers, Coordinate Measuring Machines etc. [3, 4, 5, 6, 7]. There are also alternatives, for example use of machine vision. From the comparison of these methods in Table 1, it is clear that machine vision is a suitable alternative for such measurements. But so far it was difficult to make six dimensional measurements, especially the orientation measurements. For such measurements on a robot, typically a stereo vision set-up is required. This means that two calibrated cameras are to be used [8], which has issues related to the field of view due to limited overlap of both the views. Additionally, there is issue of correspondence as well. This is not the case for a monocular camera. But the issue is that six dimensional pose measurements are not directly possible unless the camera is pre-calibrated [9, 10]. It needs to be noted that a major roadblock for using camera based measurements in robot identification is that due to limited depth of focus, the workspace size is significantly reduced thus affecting kinematic identification of industrial robots which have significantly bigger work space. To use camera based measurements in this situation, there might be need for multiple changes in focal length for making measurement in different regions of the workspace. This will make it necessary that a separate camera calibration is done before each change which is not a convenient alternative. It will be a great advantage if pose measurement can be done without the mandatory pre-calibration step as is required by artificial reality toolkit ArUco. The solution is to use the external calibration information from standard calibration methods. But all the major calibration methods require multiple images from various possible orientations for calibration. Additionally not all poses of camera is suitable for camera calibration [11]. But, while making measurements, say, to calculate repeatability, the same particular pose has to be attained multiple times [1]. Thus, there is an additional requirement that, six dimensional pose is obtained from each image captured while camera which is mounted on the robot reaches the particular pose. This means that camera should measure the pose from a single image itself. In this paper, a new method of measurement of a six dimensional pose using a single image of a monocular camera is presented. The same was applied for the measurement of performance of an industrial robot. To our knowledge, this is the first time performance measurement of a robot in six dimensions is reported using a monocular camera system. Though it is not necessary that the camera is calibrated earlier, at the end of the measurement process the camera internal parameters are also obtained. As a result in Section II we introduce the method as calibration of camera using a single image.

TABLE I COMPARISON OF DIFFERENT SENSORS FOR MEASUREMENTS (LOW- L, MEDIUM- M, HIGH- H, VERY HIGH- VH, DYNAMIC- D, STATIC- S, RESOLUTION- R, COST- C, REUSABILITY- RU, PORTABILITY-P, EASE OF USE- E, ONLINE INSPECTION- O, MEASUREMENT CHARACTERISTICS- MC, YES-Y, NO-N) (ADAPTED FROM [2]).

Sensor/Feature	R	C	RU	P	E	O	MC
Artefacts	1µm	M	N	Y	M	N	S
CMM	0.5µm	H	Y	N	H	N	S
Theodolite	5mm	M	Y	Y	M	N	S
Linear Potentiometer	10 µm	L	Y	Y	M	N	D (Low speed)
Laser Interferometry	0.16-5µm	V H	Y	Y	H	N	D
Machine vision	0.8µm	M	Y	Y	H	Y	D

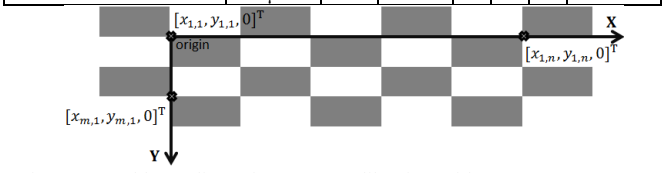

Figure 1 World coordinate frame on a calibration grid.

Organization of the paper is as follows. Section II discusses about a new camera calibration algorithm using only single image from a monocular camera. Section III discusses about 6D pose measurement using a monocular camera. In Section IV, experimental results on an industrial robot are presented. Section V discusses about the conclusions.

*Research supported by grant towards setting up of PAR lab from BARC/BRNS, India.

R A Boby and S. K. Saha are with department of Mechanical Engineering IIT Delhi.(Phone: 0091-9999050029, email: ribyab@gmail, saha@mech.iitd.ac.in)

II. SINGLE IMAGE BASED CAMERA CALIBRATION

The end-effector position of a robot mounted with an un-calibrated camera is possible if we implement an onsite calibration. This will give us the camera extrinsic parameters which in turn will define the end effector position of the robot. But the disadvantage with the existing camera calibration algorithms are that, they [12, 13, 14, 15] use multiple images to obtain camera calibration information. These formulations have opinioned that calibration from single image is not possible.

Camera calibration algorithms using single image have been reported in literature [16, 17]. In [16], a simplified intrinsic matrix was considered since very accurate measurements were not the main concern. In [17], single image based intrinsic parameter estimation was talked about. These methods will not be suitable for six dimensional pose measurement of an industrial robot thus paving way for the development of the approach discussed in this paper.

Internal parameters consist of effective focal length in x direction (f_x), effective focal length in y direction (f_y), and image coordinates of principal point (c_x, c_y). External parameters consist of rotation ($\mathbf{R}$) and translation ($\mathbf{t}$). Let $\mathbf{p}$ be the image coordinate of a point having World coordinate $\mathbf{x}$ where, $\mathbf{p} \equiv [p, q, s]^{\mathrm{T}}$ and $\mathbf{x} \equiv [x, y, z, 1]^{\mathrm{T}}$**.** The corresponding image coordinates are defined by $\mathbf{u}$**,** where, $\mathbf{u} \equiv [u, v, 1]^{\mathrm{T}}$.The transformation from Calibration grid frame to Camera frame is given by $\mathbf{T}$. Then the following expression is obtained.

$$\mathbf{p} = \mathbf{CTx} \tag{1}$$

where, $\mathbf{T}$ is the 3×4 matrix such that $\mathbf{T} \equiv [\mathbf{R}|\mathbf{t}]$ made of rotation matrix $\mathbf{R}$, translation vector $\mathbf{t}$ .The matrix $\mathbf{C}$ is of size 3×3 comprising of intrinsic parameters of the camera.

Note that, $\mathbf{R} \equiv \begin{bmatrix} r_{11} & r_{12} & r_{13} \\ r_{21} & r_{22} & r_{23} \\ r_{31} & r_{32} & r_{33} \end{bmatrix}$, $\mathbf{C} \equiv \begin{bmatrix} f_x & 0 & c_x \\ 0 & f_y & c_y \\ 0 & 0 & 1 \end{bmatrix}$. and $\mathbf{t} \equiv [t_x, t_y, t_z]^T$,

Imagine that a single image has been considered and the image coordinates $\mathbf{u}_{i,j} \equiv [u_{i,j}, v_{i,j}, 1]^T$ corresponds to a point with the coordinate $\mathbf{x}_{i,j} \equiv [x_{i,j}, y_{i,j}, z_{i,j}, 1]^{\mathrm{T}}$ from the i^{th} row and the j^{th} column of the calibration grid (Fig. 1). The homogenous image coordinates of the same point is given by $\mathbf{p} \equiv [p_{i,j}, q_{i,j}, s_{i,j}]^T$. The calibration grid is planar and has arrays of squares. Therefore $z_{i,j}$=0 $\forall\, i, j$. We take for granted that the origin is at the first cross-section point on the calibration grid (Fig. 1). If that is not the case, the origin can be translated to this particular point for the time being. Later, the reverse translation can be done to bring the final transformation as per the initial condition. There are multiple stages at which relevant equations are framed. They are as follows.

A. Considering the point at the origin of the calibration coordinate system

If the origin of the coordinate system is considered, (1) will get reduced to

$$s_{1,1}\mathbf{u}_{1,1} = \mathbf{C}[t_x, t_y, t_z]^{\mathrm{T}} \tag{2}$$

This yields two equations which are as follows.

$$u_{1,1}t_z = f_x t_x + c_x t_z \tag{3}$$

$$v_{1,1}t_z = f_y t_y + c_y t_z \tag{4}$$

$s_{1,1} = t_z$, as obtained from (2).

B. Considering the points on the x-axis

In the second stage, we consider all the points lying on the x-axis of the coordinate system. We have the following equation in that case.

$$s_{1,j}\mathbf{u}_{1,j} = \mathbf{C}\begin{bmatrix} r_{11} & t_x \\ r_{21} & t_y \\ r_{31} & t_z \end{bmatrix}\begin{bmatrix} x_{1,j} \\ 1 \end{bmatrix} \tag{5}$$

If we substitute (3) and (4) in (5), it yields the following two equations:

$$x_{1,j}\alpha + (u_{1,1} - u_{1,j})t_z - u_{1,j}x_{1,j}r_{31} = 0 \tag{6}$$

$$x_{1,j}\beta + (v_{1,1} - v_{1,j})t_z - v_{1,j}x_{1,j}r_{31} = 0 \tag{7}$$

Here, $\alpha \equiv f_x r_{11} + c_x r_{31}$ and $\beta \equiv f_y r_{21} + c_y r_{31}$. Let m be the number of rows in the grid. For multiple values ($j \subset (2, m), j \epsilon \mathbb{Z}$) the equation can be formulated as follows.

$$\mathbf{L_1}[\alpha, t_z, r_{31}, \beta\,]^{\mathrm{T}} = \mathbf{0} \tag{8}$$

Where $\mathbf{0}$ is a $2(n-1)$ dimensional vector of zeros and $\mathbf{L_1}$ is a $2(n-1) \times 4$ marix given by,

$$\mathbf{L_1} \equiv \begin{bmatrix} x_{1,2} & u_{1,1} - u_{1,2} & -u_{1,2}x_{1,2} & 0 \\ 0 & v_{1,1} - v_{1,2} & -v_{1,2}x_{1,2} & x_{1,2} \\ \vdots & \vdots & \vdots & \vdots \\ x_{1,n} & u_{1,1} - u_{1,n} & -u_{1,n}x_{1,n} & 0 \\ 0 & v_{1,1} - v_{1,n} & -v_{1,n}x_{1,n} & x_{1,n} \end{bmatrix}$$

The values of α, t_z, r_{31} and β can be obtained as,

$$[\alpha, t_z, r_{31}, \beta\,]^{\mathrm{T}} = \mathrm{null}(\mathbf{L_1}) \tag{9}$$

Since the solution is in the null-space of $\mathbf{L_1}$**,** it is of the form of a constant c multiplied by a 4 dimensional vector of real numbers. Further steps involve the solution obtained at this stage. Therefore, the parameter c will figure in all the subsequent solutions.

C. Considering the points on the y-axis

In the third stage, we consider all the points lying on the y-axis of the coordinate system. We have then the following equation:

$$s_{i,1}\mathbf{u}_{i,1} = \mathbf{C}\begin{bmatrix} r_{12} & t_x \\ r_{22} & t_y \\ r_{32} & t_z \end{bmatrix}\begin{bmatrix} y_{i,1} \\ 1 \end{bmatrix} \tag{10}$$

The parameter t_z has been obtained in the previous stage. If we substitute (3) in (9), it yields the following two equations:

$$y_{i,1}\gamma - u_{i,1}y_{i,1}r_{32} = -(u_{1,1} - u_{i,1})t_z \tag{11}$$

$$y_{i,1}\delta - v_{i,1}y_{i,1}r_{32} = -(v_{1,1} - v_{i,1})t_z \tag{12}$$

Here, $\gamma \equiv f_x r_{12} + c_x r_{32}$ and $\delta \equiv f_y r_{22} + c_y r_{32}$. Let m be the number of rows in the grid. For multiple values ($i \subset (2, m), i \epsilon \mathbb{Z}$) the equation can be formulated as follows.

$$\mathbf{L_2}[\gamma, r_{32}, \delta]^{\mathrm{T}} = \mathbf{b_2} \tag{13}$$

where $\mathbf{b_2}$ is $2(m-1)$ dimensional vector given by,

$$\mathbf{b_2} = -t_z[u_{1,1} - u_{2,1}, v_{1,1} - v_{2,1}, \ldots, u_{1,1} - u_{m,1}, v_{1,1} - v_{m,1}]^{\mathrm{T}}$$

whereas the $2(m-1)$×3 matrix $\mathbf{L_2}$ is given by

$$\mathbf{L_2} = \begin{bmatrix} y_{2,1} & -y_{2,1}u_{2,1} & 0 \\ 0 & -y_{2,1}v_{2,1} & y_{2,1} \\ \vdots & \vdots & \vdots \\ y_{m,1} & -y_{m,1}u_{m,1} & 0 \\ 0 & -y_{m,1}v_{m,1} & y_{m,1} \end{bmatrix}$$

The values of γ, r_{32} and δ are obtained next as,

$$[\gamma, r_{32}, \delta]^{\mathrm{T}} = \mathbf{L_2^{\dagger}b_2} \tag{14}$$

In (14), $\mathbf{L_2^{\dagger}}$ is the pseudo inverse of $\mathbf{L_2}$. Note that, the factor c is present in the solution of t_z. Hence, the above solution will also be a multiple of c.

D. Considering the points elsewhere

Here we consider the rest of the points. We have the following equation:

$$s_{i,j}\mathbf{u}_{i,j} = \mathbf{C}\begin{bmatrix} r_{11} & r_{12} & t_x \\ r_{21} & r_{22} & t_y \\ r_{31} & r_{32} & t_z \end{bmatrix}\begin{bmatrix} x_{i,j} \\ y_{i,j} \\ 1 \end{bmatrix} \quad (15)$$

The following two equations are obtained:

$$x_{i,j}f_x r_{11} + y_{i,j}f_x r_{12} + f_x t_x + c_x h_{i,j} = u_{i,j}h_{i,j} \quad (16)$$

$$x_{i,j}f_y r_{21} + y_{i,j}f_y r_{22} + f_y t_y + c_y h_{i,j} = v_{i,j}h_{i,j} \quad (17)$$

where $h_{i,j} = x_{i,j}r_{31} + y_{i,j}r_{32} + t_z$ (18)

which is calculated using r_{31}, r_{32} and t_z obtained from (9) and (14). For multiple points, the equations take the form given below:

$$\mathbf{L_3}[f_x r_{11}, f_x r_{12}, c_x, f_x t_x]^{\mathrm{T}} = \mathbf{b_3} \quad (19)$$

$$\mathbf{L_3}[f_y r_{11}, f_y r_{22}, c_y, f_y t_y]^{\mathrm{T}} = \mathbf{b_4} \quad (20)$$

where the $(m-1)(n-1)\times 4$ matrix $\mathbf{L_3}$ and $(m-1)(n-1)$ dimensional vectors $\mathbf{b_3}$ and $\mathbf{b_4}$ are given by

$$\mathbf{L_3} \equiv \begin{bmatrix} x_{2,2} & y_{2,2} & h_{2,2} & 1 \\ \vdots & \vdots & \vdots & \vdots \\ x_{m,n} & y_{m,n} & h_{m,n} & 1 \end{bmatrix} \text{ and}$$

$$\mathbf{b_3} \equiv [u_{2,2}h_{2,2}, \dots, u_{m,n}h_{m,n}]^{\mathrm{T}}$$

$$\mathbf{b_4} \equiv [v_{2,2}h_{2,2}, \dots, v_{m,n}h_{m,n}{}^{\mathrm{T}}]$$

Then the solutions are obtained as follows:

$$[f_x r_{11}, f_x r_{12}, c_x, f_x t_x]^{\mathrm{T}} = \mathbf{L_3^{\dagger}}\mathbf{b_3} \quad (21)$$

$$[f_y r_{21}, f_y r_{22}, c_y, f_y t_y]^{\mathrm{T}} = \mathbf{L_3^{\dagger}}\mathbf{b_4} \quad (22)$$

In (21) and (22), $\mathbf{L_3^{\dagger}}$ is the pseudo inverse of $\mathbf{L_3}$. Note that $\mathbf{b_3}$ in (19) has the common factor c. This is because all the terms r_{31}, r_{32} and t_z in (18) is a multiple of c. Therefore, the solution for all the terms except c_x and c_y in (19) and (20) were obtained as a multiple of c. The solutions to c_x and c_y are obtained from (21) and (22).

E. Estimation of rotation matrix

The solutions obtained till now can be used to obtain the rotation matrix $\mathbf{R}$. The solutions of (21) can be used to obtain

$$\frac{r_{11}}{r_{12}} = \frac{f_x r_{11}}{f_x r_{12}} = c_1 \quad (23)$$

The solutions of (22) can be used to obtain

$$\frac{r_{21}}{r_{22}} = \frac{f_y r_{21}}{f_y r_{22}} = c_2 \quad (24)$$

Since $\mathbf{R}$ is an orthonormal matrix, $\mathbf{R}^{\mathrm{T}}\mathbf{R} = \mathbf{I}$, $\mathbf{I}$ being 3×3 identity matrix. Hence, for the first and second columns of $\mathbf{R}$, one can write.

$$[r_{11}, r_{21}, r_{31}]^{\mathrm{T}}[r_{12}, r_{22}, r_{32}] = 0 \quad (25)$$

$$r_{11}^2 + r_{21}^2 + r_{31}^2 = 1 \quad (26)$$

$$r_{12}^2 + r_{22}^2 + r_{32}^2 = 1 \quad (27)$$

Consider $r_{32} = cr'_{32}$and $r_{31} = cr'_{31}$, as obtained from (9) and (13), respectively, and substituting (23) and (24) in (25)-(27) one gets the following expression,

$$\begin{bmatrix} {c_1}^2 & {c_2}^2 & {r'_{31}}^2 \\ c_1 & c_2 & r'_{31}r'_{32} \\ 1 & 1 & {r'_{32}}^2 \end{bmatrix}\begin{bmatrix} {r_{12}}^2 \\ {r_{22}}^2 \\ c^2 \end{bmatrix} = \begin{bmatrix} 1 \\ 0 \\ 1 \end{bmatrix} \quad (28)$$

The solutions are $\pm r_{12}$, $\pm r_{22}$ and $\pm c$. They amount to eight possible solutions. For each possible combination, the following expression was used to derive the last row of $\mathbf{R}$. This is owing to the fact that all the three columns are mutually orthogonal to each other.

$$[r_{13}, r_{23}, r_{33}]^{\mathrm{T}} = [r_{11}, r_{21}, r_{31}]^{\mathrm{T}} \times [r_{12}, r_{22}, r_{32}]^{\mathrm{T}} \quad (29)$$

By substituting the obtained solutions in (9), (14), (21) or (22), the values of f_x and f_y were then obtained. We can neglect those solutions where the values are negative. This finally leaves us with two options. Considering the sign of t_z, a unique and correct solution can be identified. The value of t_z should be positive given that the calibration grid is always in front of the camera. This helps us to arrive at one final combination and thus the internal calibration matrix $\mathbf{C}$ and extrinsic matrix **T.**

F. Implementation Aspects

During the implementation of the algorithm, many practical issues sprang up. One was that, the values of image points were expressed in thousands or hundreds. Meanwhile the values of coordinates are in few millimeters. Owing to the large difference in the values, the matrix $\mathbf{L_1}$ has a very high condition number. Thus, the results were error prone. To circumnavigate this issue, normalization [14] was done for both the image coordinate points and the World coordinates.

G. Adaptation considering vanishing points and initial value of image centers.

Though the algorithm discussed till this point has an advantage that principal point estimate is not required, it may not perform as good as the standard algorithms in terms of re-projection error. Therefore, the algorithm may be adapted by utilizing vanishing points of the calibration grid image.

1) Considering vanishing points: For Eqn. (5) if the vanishing points on x axis coordinate direction is considered then,

$$[u_x^{\infty}, v_x^{\infty}]^T = \lim_{x\to\infty} \boldsymbol{u} \quad (30)$$

where $[\mathrm{u_x^{\infty}}, \mathrm{v_x^{\infty}}]^T$ is the point at infinity on x axis. Similarly, for vanishing points on y axis,

$$[u_y^{\infty}, v_y^{\infty}]^T = \lim_{x\to\infty} \boldsymbol{u} \quad (31)$$

If this condition is introduced in Eqn. 8, we can obtain t_z and r_{31} directly. Using the value of r_{31}, the following expressions are also obtained.

$$\alpha = r_{31}\mathrm{u_x^{\infty}} \quad (32)$$

$$\beta = r_{31}\mathrm{v_x^{\infty}} \quad (33)$$

Similarly, utilizing (31), (13) yields a solution for r_{32}. The following expressions also are obtained:

$$\gamma = r_{32}\mathrm{u_y^{\infty}} \quad (34)$$

$$\delta = r_{32}\mathrm{v_y^{\infty}} \quad (35)$$

2) *Using Orthonormal conditions*: The fact that rotation matrix is orthonormal can be used to deduce expressions for solving c_x, c_y, f_x and f_y. In [12], it is recommended to use an initial estimate of c_x and c_y for calibration using single image. Therefore, using an initial estimate of c_x and $\mathrm{c_y}$ all the required parameters were estimated. Distortion parameters were also estimated as stated in Section IIH. This method is more numerically stable than the other one because there are no matrix inversions. This implies conditioning of the matrices is not a problem. Therefore,

there is no need to scale and shift the data during calibration process.

H. Distortion model and Parameter Optimization

After the initial estimates of camera parameters were obtained the corresponding distortion parameter were calculated. At the final stage all the estimated parameters were optimized to minimize the re-projection error. This is similar to the approach in [12].

III. Pose Measurement

Robot calibration and performance measurement can be done by mounting the camera on the end-effector of the robot. In this case, the transformation $\mathbf{T}$ is from camera coordinate system to World coordinate system (Fig. 2a). To find out the pose of camera on the end-effector, the following expressions can be used.

$$\mathbf{p}_{ee} = -\mathbf{R}^{\mathrm{T}}\mathbf{t}_{\boldsymbol{n}} \quad (36)$$

$$\mathbf{R}_{\boldsymbol{ee}} = \mathbf{R}^{\mathrm{T}} \quad (37)$$

where, $\mathbf{p}_{ee}$ is the position of the end-effector with respect to the World coordinate system defined in the calibration grid. The matrix, $\mathbf{R}_{\boldsymbol{ee}}$ the orientation of the end-effector with respect to World coordinate frame. This can be converted to roll (α), pitch (β) and yaw (γ) angles since most of the industrial robot controllers express orientation in terms of these [18].

TABLE II COMPARISON OF REPROJECTION ERRORS OF PROPOSED ALGORITHM.[1]

Algorithm	Re-projection Errors (Pixels)	Standard deviation (Pixels)
Zhang, 2000 [9]	0.897	0.13
Proposed	0.8629	0.079

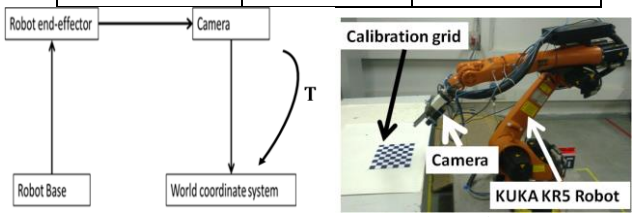

(a) (b)

Figure 2 (a) Transformations between coordinate systems.(b) Camera mounted on the end-effector and calibration grid

The major application for the proposed camera calibration algorithm discussed in Section II is with regard to the measurement of the performance of an industrial robot, especially repeatability and accuracy [1, 2]. Both these require the robot to repeatedly go to the same commanded pose. For each pose of a robot, the camera mounted on the end-effector will be able to capture an image which can be used to derive the pose of the robot. In such case, this algorithm will come handy since the pose can be extracted from a single image corresponding to a single given pose.

Another application of the proposed pose estimation is kinematic identification. One methodology is to rotate each link keeping the other ones stationary and then making the measurements of the end-effector's pose. This is called Circle Point Analysis (CPA) in calibration literature [19]. A major issue during this process is that the calibration grid might go out of focus for a given lens system. An advantage of the single image based camera calibration method is that during robot calibration the end-effector pose measurement can be made by even adjusting the focal length. If conventional calibration algorithm [20, 21] based on differential errors is considered, the observability [22, 20, 23] of kinematic parameters gets enhanced when measurements of orientation is also made. Here again camera based measurement will have an edge since the orientation data can be obtained easily without extra attachments on the end-effector. For more discussion about calibration methodologies see Appendix A.

Currently the trusted method of performance measurement and kinematic parameter identification is based on Laser Trackers [24, 25, 26, 27]. But as discussed in Section I, a vision system has a host of advantages if it can be used appropriately. The performance of the algorithm and pose estimation will be discussed in Section IV.

It may be noted that the performance measurement and CPA based methods do not need eye-to-hand calibration. Therefore, this aspect is omitted in the current paper. The quantities $\mathbf{p}_{ee}$ and $\mathbf{R}_{\boldsymbol{ee}}$ are considered as to represent the end-effector position and orientation, respectively, since the camera is rigidly mounted on the end-effector. But for measuring absolute accuracy of the end-effector this may be obtained by any of the eye-to-hand calibration algorithms available in the literature.

IV. Experimental Results and Discussions

The performance was evaluated in two stages. In the first stage, camera calibration algorithm was compared with other calibration algorithms. At the later stage, the camera was mounted on the KUKA KR5 Arc robot, as shown in Fig. 2b. After that, pose measurements were made and comparison was done with the data obtained from Artificial Reality Toolkit ArUco.

A. Results of Camera Calibration using Single Image

Initially, single image was captured using Basler Pilot camera with 8mm lens and resolution 2448×2050 pixels. The calibration grid points were detected using OPENCV [9]. Camera calibrations were done using both the Zhang's [12] algorithm and the methodology proposed in Section II. The re-projection errors for the two methods are shown in Table II. The proposed algorithm outperforms Zhang's algorithm with respect to both re-projection error and standard deviation of it. Zhang's algorithm was based on the implementation given in [28]. This implementation requires minimum of two images to run. It is also worth noting that the proposed algorithm outperformed Zhang's algorithm with only one image as input. Zhang's algorithm was highly dependent on the pose of the camera and the calibration grid, whereas the proposed algorithm was not affected much by the pose. Proposed method could yield results even in camera poses where Zhang's algorithm could not give results.

Tsai's algorithm [13] has a similar formulation but has the disadvantage that it fails when optical axis is perpendicular to the calibration grid. The only other paper in the literature which discusses camera calibration using single image is [16]. Our results cannot be compared with [16] as rotation matrix representation might be subject to singularity since roll, pitch, yaw angles were directly considered. Also the model is highly simplified. Additionally, the errors reported are far too high for the application discussed in this paper.

[1] The resolution of camera is 2448×2050 and total number of images is 10

B. Comparison of Robot's Pose Estimation

1) Performance measurement: Experiments were performed for measuring the robot's repeatability. This was done according to ISO9283 [1, 2]. A cube was defined of size 100mm×100mm×100mm. Five points were defined and end-effector was made to move from one position to the next position within the cube. At each position, calibration grid image was taken. The robot's positions similar to the ones shown in Fig. 2b were measured. The experiment was conducted at 30% speed of the robot. For the same experimental conditions, measurements were taken using ArUco [10] to enable comparison of pose measurement systems which uses camera. The camera was first calibrated using OPENCV. Later this calibration values were used in the ArUco pose detection algorithm.

Table III shows the comparison of results of repeatability. The technical specification of KUKA KR5 Arc (KRC2 controller) claims a repeatability of 0.1mm. The results obtained from the proposed method are closer to the original specification of the robot compared to those obtained using ArUco. Table III shows the repeatability of the same robot in six dimensions with 30% speed. Please note that we were able to capture information about orientation repeatability in this study. The largest value obtained using the proposed method is about 0.026º whereas that obtained using ArUco is 0.4º. Though we do not have correct technical measures from the robot manufacturer, it may be understood that the ability to measure lower values of orientation repeatability is an advantage. Thus the proposed method is better in this regard. Therefore, in both position and orientation measurements, the proposed method fares better. Additionally, there is no need to calibrate the camera separately as in the case of ArUco. Calibration and pose measurements are achieved in single step.

To make similar measurements, expensive mountings are to be attached to the end-effector with multiple retro-reflectors so that measurements with laser tracker are possible. Orientation repeatability in spite of being laid down in ISO 9283 is not specified by robot manufacturers. In such situations, camera-based measurements are a suitable option. This is the first instance in literature where performance measurements have been made using a camera-based system. Earlier such measurements were done using special set-ups [22, 40]. Multi-view based methods [30, 31]cannot be used for these experiments because of the reason discussed in Section I. These results are a significant improvement over the results discussed in [32].

2) Kinematic parameter identification: Over the years starting from 1990's researchers have been talking about using camera for robot parameter identification. Many of these studies have derived the analytical expressions but did not support with experimental studies [8, 33]. Experimental studies related to positioning accuracy improvement have been reported in [30, 31]. Both of these methods require multiple views for making the final measurement. Identified values of kinematic parameters or comparison with the state of the art measurement methods also are lacking. For example, [20] talks about experimental studies for parameter identification of MCPC parameters. But most of the industrial robots use the Denavit Hartenberg (DH) model [34] and thus it will be more suitable to implement kinematic identification using this model. In the current study, DH model parameters have been identified using the Circle Point Analysis [35]. Two calibration grids placed mutually perpendicular to each other have been used during measurements stage. The identification results are given in Table IV. A detailed explanation about identification procedure will be included in a future version of the paper.

TABLE III. COMPARISON OF REPEATABILITY FOR KUKA KR5 ARC ROBOT

Algorithm/Pose		P1	P2	P3	P4	P5
Proposed	Position (mm)	0.258	0.157	0.330	0.218	0.307
	Roll (deg)	0.014	0.008	0.007	0.007	0.008
	Pitch (deg)	0.026	0.011	0.016	0.015	0.023
	Yaw (deg)	0.017	0.012	0.018	0.014	0.018
ArUco	Position (mm)	0.386	1.376	1.764	1.591	0.862
	Roll (deg)	0.052	0.061	0.198	0.030	0.034
	Pitch (deg)	0.069	0.357	0.278	0.456	0.057
	Yaw (deg)	0.147	0.226	0.437	0.181	0.271

TABLE IV IDENTIFIED VALUES FOR KUKA KR5 ARC ROBOT

Link		1	2	3	4	5
Identified	α (°)	77.6	2.4	94.9	94.2	90.9
	a(mm)	189.6	759.4	105.9	271.5	30.1
	b (mm)	0	0	173.7	44.0	9.2

V. CONCLUSIONS

This paper discusses about six dimensional pose measurements using a single image-based calibration of a monocular camera. This is of significance in the performance measurement and kinematic parameter identification of an industrial robot. The end–effector's pose in six dimensions can be obtained using this calibration data. Later, experimental studies for measuring repeatability were conducted on a KUKA KR5 ARC robot using the proposed method. Comparisons with pose measurement using ArUco was also made. The results reveal that the proposed method was able to perform better than ArUco based measurement. The measured values are closer to the technical specifications laid down by the robot manufacturer. Note that ArUco requires an initial camera calibration stage, which is not necessary in the proposed method. Especially in orientation measurement, camera-based method has an upper hand since six dimensional measurements were possible without mounting any high precision artefact at the end-effector as is required while using laser trackers. It is also worth noting that measurement systems like CMM and laser trackers are bulky and offline

Though the main purpose of the algorithm is pose measurement, the algorithm can also be used for calibration of camera from a single image, whereas all the major algorithms need multiple images for calibration. The performance of the calibration algorithm is better than that obtained from Zhang's algorithm.

APPENDIX A

In kinematic parameter identification, the optimization based

methods have issues with observability of parameters [36, 37, 38]. This is not so for CPA based method which is based on Chasles theorem [20, 24]. The relative orientation, distances etc. between the vectors representing two nearby joints can be measured to find out the total kinematic parameters. In Fig. 3, two lines represent the joint axis for i^{th} and $i+1^{th}$ link. The direction cosines, Points C,D and G are calculated. The algorithm based on SVD [39] was used to derive these parameters from the 3D pose trajectory for two nearby links measured using camera. Link length, Twist angle and Joint offset were then obtained.

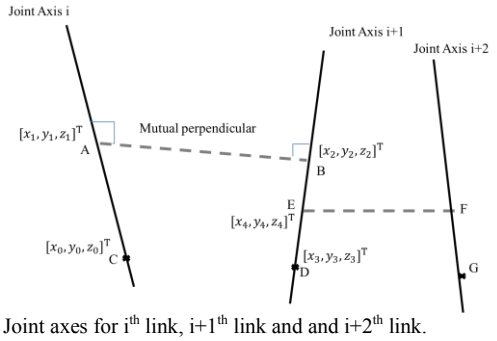

Figure 3 Joint axes for i^{th} link, $i+1^{th}$ link and and $i+2^{th}$ link.

ACKNOWLEDGMENT

We thank Mr. A. A. Hayat for the help in doing experiments.

REFERENCES

[1] Manipulating industrial robots —performance criteria and related test methods, ISO 9283, 1998.

[2] Manipulating Industrial Robots - Informative Guide on Test Equipment and Metrology Methods of Operation for Robot Performance Evaluation in Accordance with ISO 9283, ISO 13309, 1995.

[3] M. R. Driels, W. Swayze and S. Potter, "Full-pose calibration of a robot manipulator using a coordinate-measuring machine", *Int. J. Adv. Manuf. Technol.*, Volume 8, Issue 1, pp 34-41, 1993.

[4] W. S. Newman, C. E. Birkhimer and R. J. Horning, "Calibration of a Motoman P8 Robot Based on Laser Tracking", *Proc. 2000 IEEE ICRA.*, pp. 3597-3602, 2000.

[5] G. R. Tang and L.S. Liu, "Robot calibration using single laser displacement meter", *Mechatron.*, vol. 3, pp. 503-516, 1993.

[6] K. Lau, R. Hocken and L. Haynes, "Robot performance measurements using automatic laser tracking techniques", *Robot. Comput. Integ. Manuf.*, vol. 2, pp. 227-236, 1985.

[7] M. Vincze, J.P. Prenninger and H. Gander, "A Laser tracking system to measure position and orientation of robot end-effectors under motion", *Int. J. of Robot. Research*, vol. 13, pp. 305-314, 1994.

[8] D. J. Bennet, D. Geiger and J. M. Hollerbach, "Autonomous calibration for hand eye coordination", *Int. J. of Robot. Research*, vol.10, pp. 550-559, 1991.

[9] "Camera Calibration and 3D Reconstruction: solvePnP.", Internet: http://docs.opencv.org/modules/calib3d/doc/camera_calibration_and_3d_reconstruction.html, [Feb. 5, 2015].

[10] Garrido-Jurado, S., Muñoz-Salinas, R., Madrid-Cuevas, F. J.and Marín-Jiménez, M. J., "Automatic generation and detection of highly reliable fiducial markers under occlusion", *Pattern Recognition*, Vol. 47, No. 6, pp.2280-2292, 2014.

[11] A. Richardson, J. Strom, E. Olson, AprilCal: Assisted and repeatable camera calibration, *2013 IEEE/RSJ IROS* , pp.: 1814–1821.

[12] Z. Zhang, "A flexible new technique for camera calibration", *IEEE Trans. Pattern Anal. Mach. Intell.*, vol. 22, no. 11, pp.1330-1334 2000.

[13] R. Y. Tsai, "A versatile camera calibration technique for high accuracy 3D machine vision metrology using off the shelf TV cameras and lenses", *IEEE J. Robot. Autom.*, vol, RA-3, no. 4, pp. 323-344, 1987.

[14] R. Hartley and A.Zisserman, *Multiple View Geometry in Comput. Vision*, Cambridge University Press, Cambridge 2001.

[15] AbdelAziz, I. Y. and Karara, H. M., Direct linear transformation into object space coordinates in close-range photogrammetry, *Proc. Symp. Close-Range Photogrammetry*, pp. 1-18, 1971.

[16] I. Miyagawa; H. Arai; H. Koike, "Simple Camera Calibration From a Single Image Using Five Points on Two Orthogonal 1-D Objects," *IEEE Trans. Image Process.* vol.19, no.6, pp.1528-1538, 2010.

[17] F. Zhou, Y. Cui, H. Gao, Y. Wang, "Line-based camera calibration with lens distortion correction from a single image", *Optics Lasers in Eng.*, Vol. 51, No. 12, pp. 1332-1343. , 2013.

[18] S. K. Saha, *Introduction to Robotics*, Tata McGraw-Hill, New Delhi, 2008.

[19] Z . S. Roth, B. W. Mooring and B. Ravani, "An overview of robot calibration", *IEEE J. of Robot. Autom.*, vol. RA3, no. 5, pp. 377-385, 1987.

[20] H. Zhuang, Z. S. Roth, *Camera-aided robot calibration*, Boca Raton : CRC Press, 1996.

[21] E. Dombre and W. Khalil, *Robot Manipulators modelling, performance analysis and control*, ISTE, London, UK, 2007

[22] J.F.Brethe, E.Vasselin,D.Lefebvre and B.Dakyo, "Determination of the Repeatability of a Kuka Robot Using the Stochastic Ellipsoid Approach", *Proc. of ICRA,* pp .4339 – 4344, 2005.

[23] J Borm and C. Meng "Determination of Optimal Measurement Configurations for Robot Calibration Based on Observability Measure", *Int. J. Robot. Research*, vol. 10, no. 1,pp. 51-63,1991

[24] R. M. Murray, Z Li and S. S. Sastry, *A mathematical introduction to robotic manipulation*, CRC Press, 1994

[25] V. Lertpiriyasuwat and M. C. Berg, "Adaptive real-time estimation of end-effector position and orientation using precise measurements of end-effector position", *IEEE Trans. Mechatron.* , Vol.11 , No 3, pp. 304 – 319, 2006.

[26] J. Santolaria, J. Conte, M. Ginés, "Laser tracker-based kinematic parameter calibration of industrial robots by improved CPA method and active retroreflector", *Int. J. of Adv. Manuf. Technol.*, vol. 66, no. 9-12, pp 2087-2106, 2013.

[27] Y. Sun and J. M. Hollerbach, "Observability Index Selection for Robot Calibration", *2008 IEEE ICRA.*, pp. 831-836, 2008.

[28] Z. Zhang, (2000), *A Flexible New Technique for Camera Calibration,*[online]. Available: http://research.microsoft.com/en-us/um/people/zhang/Calib/

[29] Jorge Santolaria, Manuel Ginés, "Uncertainty estimation in robot kinematic calibration", *Robot. Comput.-Integ. Manuf.*, vol. 29, No. 2, pp. 370–384, 2013.

[30] Y. Meng, H. Zhuang, "Self-Calibration of Camera-Equipped Robot Manipulators", *Int. J. Robot. Research*, vol. 20, pp. 909-921, 2001.

[31] J. M. S. T. Motta, G. C. de Carvalho, R.S. McMaster, "Robot calibration using a 3D vision-based measurement system with a single camera", *Robot. Comput. Integ. Manuf.*, vol. 17, pp. 487–497, 2001.

[32] P. Tiwan, R. A. Boby, S. Dutta Roy, S. Chaudhury, S. K. Saha, "Cylindrical Pellet Pose Estimation in Clutter using a Single Robot Mounted Camera", *Proc. of Conf. on Advances In Robot.*, 1-6, 2013

[33] Rousseau, P., Desrochers, A. and Krouglicof, N., "Robot Parameter Identification with Vision System Measurement," *IEEE Trans. Robot. Autom.*, Vol. 17, No. 6, pp. 972-978, December 2001.

[34] J . Denavit and R. Hartenberg, "A kinematic notation for lower pair mechanisms based on matrices", *ASME J. Applied Mechanics*, vol. 77, pp. 215-221, 1955.

[35] B. Mooring, Z. Roth and M. Driels, Fundamentals of Manipulator Calibration, John Wiley, 1991.

[36] J. Hollerbach, W. Khalil and M. Gautier, "*Model identification", in Springer Handbook of Robotics*, Inc. Secaucus, NJ, Springer-Verlag New York, 2008, ch.14, pp-321-344.

[37] W. Khalil and E. Dombre, *Modeling, Identification and Control of Robots*, Butterworth Heinemann, 2004.

[38] M. R. Driels and U. S. Pathre, "Significance of observation strategy on the design of robot calibration experiments", *J. Robot. Syst.*, vol. 7, no. 2,pp. 197–223, 1990.

[39] A. A. Hayat, R. G. Chittawadigi, A. D. Udai, S. K. Saha, "Identification of Denavit-Hartenberg Parameters of an Industrial Robot", AIR '13 *Proc. Conf. on Advances In Robot.*, pp. 1-6, 2013.

[40] A. Nubiola, I. A. Bonev, "Absolute calibration of an ABB IRB 1600 robot using a laser tracker", *Robot. Comput.-Integ. Manuf.*, vol. 29,pp. 236–245, 2013.